Characteristics of 3 band orthogonal wavelet system

Dual Degree Dissertation

Submitted in partial fulfilment of the requirements for the degree of
Bachelor of Technology and Master of Technology

by

Mayur Nawal
08d07003

Supervisor
Prof. Vikram Gadre

Electrical Engineering Department
Indian Institute of Technology Bombay

May 2013

Approval Sheet

This dissertation entitled **Characteristics of 3 band orthogonal wavelet system** by Mayur Nawal (08d07003) is approved for the dual degree of Bachelor of Technology and Master of Technology in Electrical Engineering with specialization in Communication and Signal Processing.

External Examiner
Dr. Kushal Tuckley
(Retd.)Senior Scientist, 'SAMEER', IIT Bombay

Internal Examiner
Prof. (Ms.) Preeti Rao
Dept. of Electrical Engg., IIT Bombay

Guide
Prof. Vikram M. Gadre
Dept. of Electrical Engg., IIT Bombay

Chairman
Prof. E. Chandrasekhar
Dept. of Earth Sciences, IIT Bombay

Date: June 05, 2013

Place: IIT Bombay

Declaration of Academic Ethics

I declare that this written submission represents my ideas in my own words and where others' ideas or words have been included, I have adequately cited and referenced the original sources. I declare that I have properly and accurately acknowledged all sources used in the production of this thesis.

I also declare that I have adhered to all principles of academic honesty and integrity and have not misrepresented or fabricated or falsified any idea/data/fact/source in my submission. I understand that any violation of the above will be a cause for disciplinary action by the Institute and can also evoke penal action from the sources which have thus not been properly cited or from whom proper permission has not been taken when needed.

Date: .....

Mayur Nawal

(Roll No. 08d07003)

Abstract

The trigonometric parameterization of 3 band filter banks that we have used imposes a level of similarity in the variation of the Time Bandwidth Product (TBP/TFP) across its input parameters. Understanding this similarity and the similarity between the variation of TFP for Scaling and Wavelet function, we have devised a way to obtain the filter coefficients of the analysis side filter banks that leads to least value of TFP and hence giving us highly localized wavelets.

The parameterization imposes a regularity of order 1 on all the filter coefficients and hence to further differentiate between the smoothness of the scaling functions we used the Sobolevs smoothness measure. Learning from his idea and understanding the major characteristics of the scaling function, we devised a new method to calculate the smoothness of the scaling functions and our results provides wavelets that seem more smooth that the once obtained from the Sobolevs criteria.

Acknowledgements

I would like to thank my awesome guide,Prof. Vikram M Gadre, for his wonderful guidance and support. His mentorship has been a major force in reviving my interst in academics and research. His inputs during our discussions have been very valuable. Not only at the academic level but also at personal level i have learned a lot from him and will look forward to his continuous guidance in future.

I am thankful to Mr. Dinesh Bhati for his support and encouragement. He has been a wonderful friend and guide to me.

I Would also like to thank all TI-DSP lab members, at IIT Bombay, Prateek Chaplot, Sanket Deshmukh, Manish Sharma, Rohanil Raje, Venkateswararao Cherukuri, Keerthi, Abhishek, Venkateshwara Reddy, Aniket P, Abrar, Ankit, Chinmay Marathe, Bishwa kalyan, Harshad, Atishay and Shubhanga who helped me resolving various issues faced in research and to maintain lab.
I would like to express my deep gratitude towards my batchmates, Amogh 'bamog' Garg, Pravjyot 'Muchad' Singh Deogan, Vivek 'Naatu' Shivade, Vashist 'Gulti' Avadhanula for helping me out in solving the difficult parts of my project.
I would like to thank all my friend and team mates for being awesome and giving me wonderful memories to take back.
Finally, I would like to thank my Parents and my brother for their support and blessings.

Contents

List of Figures

List of Tables

Chapter 1

Introduction

1.1 Literature Review

Various techniques like eigenvalue decomposition, state space manifestation, Smith McMillan, dyadic based factorizations has been developed to design Unitary, Paraunitary and Lossless M band wavelet systems ([1]:660-775)- [5]. Extending the above designs many authors have designed M band orthogonal system [6] - [11]. Algebraic approaches to develop these M-band system have been explained in [9], [12], [13]. The theory and design of Wavelets and filter banks has been explained in [14] - [16]. From the perspective of using wavelets in applications many parameters of the wavelet systems are studied and optimized, namely: perfect reconstruction, orthonormality, symmetry, regularity (smoothness), frequency selectivity, coding gain [2] - [11], [16] - [20]. Extending the work on M band wavelet systems research has also been done in the field of rational sampling and Modified M band wavelet systems [20] - [21]. Encompassing the work of I. Daubechies for imposing regularity on 2 band systems, work has been done to structurally impose regularity on wavelet system [2] - [3]. Methods to improve time-frequency resolution for orthonormal and biorthogonal wavelet systems have been discussed in [7], [8], [10]. Extending this work we are trying to study the TFP property of filter bank and trying to relate it to symmetry, frequency selectivity and regularity for 3 band orthonormal wavelet systems.

1.2 Abstract

In literature there has been considerable amount of work done in relating the various properties of a M (2) channel filter bank like Orthonormality, Paraunitariness, Regularity (Vanishing Moments), Convergence and Frequency Selectivity. There has however

been very little discussion about how to relate the above parameters with the Time Frequency Product (TFP) or Time Bandwidth Product (TBP). In the following report we have first implemented an orthonormal 3 band wavelet system. Following it we have studied the sets of this wavelet system which gives us low TFP, symmetry, good frequency selectivity and good regularity respectively. We have followed it up with forming a correlation of the scaling and wavelet functions for 3 band case. We concluded the report by stating the relation between TFP, frequency selectivity and regularity. All the concepts used in the designs are explained with an example and have been included at appropriate places along with the relevant reference materials.

Chapter 2

Basic Concepts

2.1 Paraunitary matrix

The analysis and synthesis filters of 3 channel filter banks can be expressed in terms of the polyphase matrices $E(z)$ and $R(z)$. If the filters are of finite length and satisfy perfect reconstruction (P.R) property, then the determinant of $E(z)$ must be a delay[[]:238]. This ensures a finite length $R(z)$ satisfying P.R. If $E(z)$ satisfies paraunitary property, then it ensures that its determinant is a delay, hence ensuring a P.R filter bank. Paraunitariness is not a necessary condition for $E(z)$ to be a delay; this is because it is a stronger condition then P.R condition. A transfer matrix is said to be paraunitary if :

$$\tilde{E}(z)E(z) = cI, \quad \text{for all z} \tag{2.1}$$

$$\tilde{E}(z) = E_*^T(z^{-1}) \tag{2.2}$$

Here $*$ refers to the operation of conjugating the coefficient without changing z.

An Example to illustrate this concept:
Let $c = 1$, we will create a 3×3 paraunitary matrix of degree 2, as follows:

$$V_i(z) = I - v_i v_i^T + z^{-1} v_i v_i^T \tag{2.3}$$

where v_i are 3×1 column vector with unit norm and v_i^T is the transpose of v_i.

$V_i(z)$ are degree one matrix that satisfies paraunitary property.

Any degree 2 FIR paraunitary $E(z)$ can be expressed as:

$$E(z) = V_2(z)V_1(z)U \tag{2.4}$$

Where U is a constant unitary matrix given by,

$$U = U_1 U_2 D \tag{2.5}$$

$$U_i = I - 2u_i u_i^T \quad \text{is Householder matrix}, i \in \mathbb{Z} \tag{2.6}$$

Here u_i is a 3×1 column vector with unit norm and D is a diagonal matrix given by:

$$D_{ii} = e^{j\alpha_i} \quad \alpha \text{ is real} \tag{2.7}$$

$$v_i \,/\, u_i = \begin{pmatrix} cos(\theta_1)cos(\theta_2) \\ cos(\theta_1)sin(\theta_2) \\ sin(\theta_1) \end{pmatrix} \tag{2.8}$$

Using the above equations, all set of paraunitary 3×3 transfer matrices can be formed.

2.2 Polyphase Decomposition

Consider a filter

$$H(z) = \sum_{n=-\infty}^{\infty} h(n) * z^{-Ml} \tag{2.9}$$

We can write it as a sum of M polyphase components as in equation 2.10 and 2.12:

$$H(z) = \sum_{l=0}^{M-1} z^{-l} E_l(z^M) \tag{2.10}$$

$$E_l(z^M) = \sum_{n=-\infty}^{\infty} h(Mn + l) z^{-n} \tag{2.11}$$

$$H(z) = \sum_{l=0}^{M-1} z^{(-M-1-l)} R_l(z^M)) \tag{2.12}$$

$$R_l(z^M) = \sum_{n=-\infty}^{\infty} h(M(n+l) - (l+1)) z^{-l} \tag{2.13}$$

Following example illustrates this concept :
Let $h(n) = h(0) = 1, h(1) = 2, h(2) = 3, h(3) = 4, h(4) = 5, h(5) = 6$ be a length 6 filter.
We will decompose it into 3 polyphase components as using above equations:
Method 1 :

$$H(z) = \sum_{l=0}^{2} z^{-l} E_l(z^3) \tag{2.14}$$
$$E_0(z) = 1 + 4 * z^{-1} \tag{2.15}$$
$$E_1^3(z) = 2 + 5 * z^{-1} \tag{2.16}$$
$$E_2^3(z) = 3 + 6 * z^{-1} \tag{2.17}$$
$$H(z) = z^0(1 + 4 * z^{-3}) + z^{-1}(2 + 5 * z^{-3}) + z^{-2}(3 + 6 * z^{-3}) \tag{2.18}$$
$$H(z) = 1 + 2 * z^{-1} + 3 * z^{-2} + 4 * z^{-3} + 5 * z^{-4} + 6 * z^{-5} \tag{2.19}$$

Method 2 :

$$H(z) = \sum_{l=0}^{2} z^{(-2-l)} R_l(z^3)) \tag{2.20}$$
$$R_0(z) = 3 + 6 * z^{-1} \tag{2.21}$$
$$R_1(z) = 2 + 5 * z^{-1} \tag{2.22}$$
$$R_2(z) = 1 + 4 * z^{-1} \tag{2.23}$$
$$H(z) = z^{-2}(3 + 6 * z^{-3}) + z^{-1}(2 + 5 * z^{-3}) + z^0(1 + 4 * z^{-3}) \tag{2.24}$$
$$H(z) = 1 + 2 * z^{-1} + 3 * z^{-2} + 4 * z^{-3} + 5 * z^{-4} + 6 * z^{-5} \tag{2.25}$$

2.3 McMillan degree

The Degree (McMillan Degree) of a causal rational system $H(z)$ is the minimum no. of delays required to implement it.
Consider an Nth order causal FIR filter

$$H(z) = \sum_{n=0}^{N} h(n) z^{-n} \quad h(N) \neq 0 \tag{2.26}$$

Therefore the degree is equal to the order N, because precisely N delays will be required to implement it.

Degree is not defined for non-causal systems because they cant be implemented by using delays alone. Degree for Single Input Single Output (SISO) causal rational system is equal to the order of the system. Degree for Multiple Input Multiple Output (MIMO) causal system is equal to the order of the Determinant of the FIR system.Degree of a system can be calculated as the order of its determinant.

Following example illustrates this concept :
Consider a causal filter :

$$H(z) = z^{-1}I \tag{2.27}$$

$$H(z) = \begin{bmatrix} z^{-1} & 0 \\ 0 & z^{-1} \end{bmatrix} \tag{2.28}$$

Here,

$$order(H(z)) = 1 \tag{2.29}$$

$$| H(z) | = z^{-2}, \quad \text{hence order of determinant} = 2 \tag{2.30}$$

$$Degree = 2 = 2 \tag{2.31}$$

Figure 2.1 gives the graphical implementation of $H(z)$, where U_0, U_1 are inputs and Y_0, Y_1 are the outputs

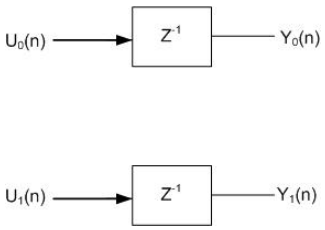

FIGURE 2.1: Implementation of filter H(z) as in Eqn. 2.27

Chapter 3

3 Band Filter Banks

In this section we will study the various properties that will help us in developing parameterizations of 3 band orthogonal wavelet system.

3.1 Ideal 3 band filter bank

A general structure of how a 3 channel filter bank works is shown in figure 3.1

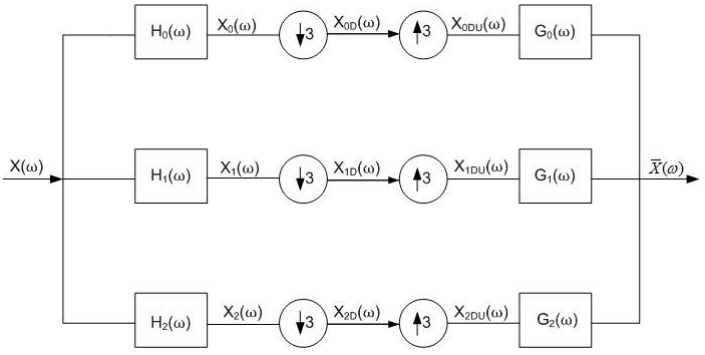

FIGURE 3.1: 3 band filter bank analysis

For the ideal 3 band filters, figure 3.1 shows the analysis and synthesis filters

The output of a perfectly reconstructed signal from a filter bank is shown in Eqn. 3.1, where we note that a change in delay and amplitude is acceptable:

$$\bar{X}(e^{j\omega}) = e^{-j\omega\tau}(A * X(e^{j\omega})) \tag{3.1}$$

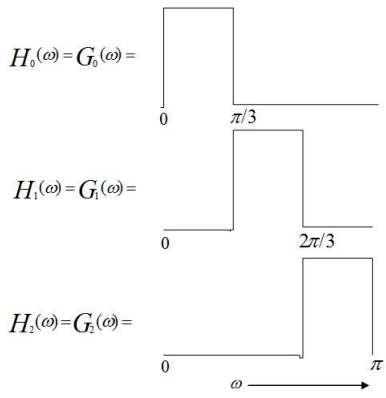

FIGURE 3.2: Analysis and synthesis filters of ideal 3 band system

Following are the outputs obtained at each stage of the filter banks :

$$X_0(e^{j\omega}) = H_0(e^{j\omega})X(e^{j\omega}) \tag{3.2}$$

$$X_1(e^{j\omega}) = H_1(e^{j\omega})X(e^{j\omega}) \tag{3.3}$$

$$X_2(e^{j\omega}) = H_2(e^{j\omega})X(e^{j\omega}) \tag{3.4}$$

$$X_{0D}(e^{j\omega}) = \frac{1}{3} * \sum_{k=0}^{2} X_0\left(e^{\frac{j\omega}{3}} e^{\frac{j2\pi k}{3}}\right) \tag{3.5}$$

$$X_{1D}(e^{j\omega}) = \frac{1}{3} * \sum_{k=0}^{2} X_1\left(e^{\frac{j\omega}{3}} e^{\frac{j2\pi k}{3}}\right) \tag{3.6}$$

$$X_{2D}(e^{j\omega}) = \frac{1}{3} * \sum_{k=0}^{2} X_2\left(e^{\frac{j\omega}{3}} e^{\frac{j2\pi k}{3}}\right) \tag{3.7}$$

$$X_{0DU}(e^{j\omega}) = X_{0D}(e^{j3\omega}) \tag{3.8}$$

$$X_{1DU}(e^{j\omega}) = X_{1D}(e^{j3\omega}) \tag{3.9}$$

$$X_{2DU}(e^{j\omega}) = X_{2D}(e^{j3\omega}) \tag{3.10}$$

$$\tag{3.11}$$

$$\bar{X}(e^{j\omega}) = G_0(e^{j\omega})X_{0DU}(e^{j\omega}) + G_1(e^{j\omega})X_{1DU}(e^{j\omega}) + G_2(e^{j\omega})X_{2DU}(e^{j\omega}) \tag{3.12}$$

Figure 3.3 shows an example of the output sequences obtained at various stages of the filter bank :

Key Note:

Here it is important to note that these ideal filters(as shown in figure 3.2) cannot be realized practically as they are of infinite length. This can be explained as follows :

Let $x_0(n)$, be the time domain sequence corresponding to the ideal filter $X_0(e^j\omega)$. Then by inverse discrete fourier transform, $x_0(n) = (2/n) * sin(n\pi/3)$, which is an infinite

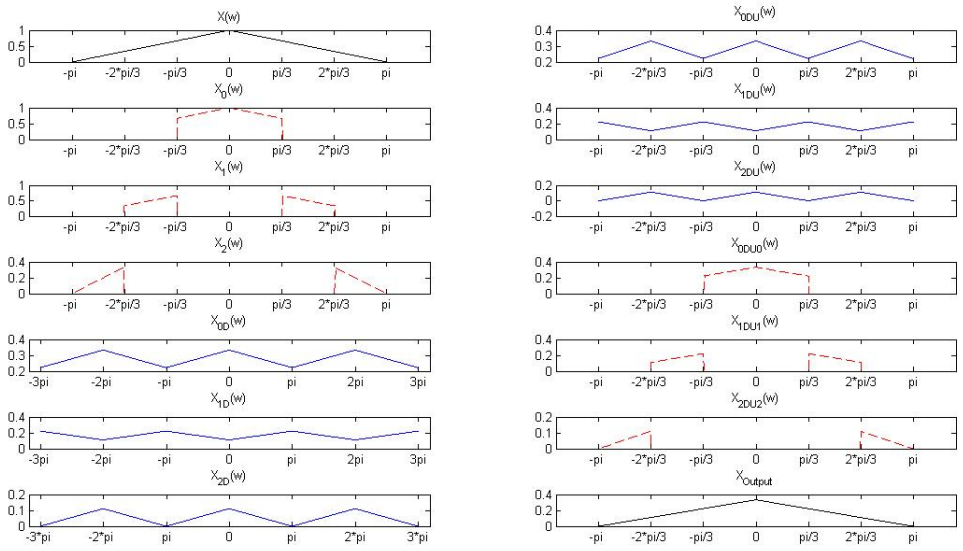

FIGURE 3.3: Example showing how an ideal filter bank works

length sequence. Similarly $x_1(n)$ and $x_2(n)$ are also infinite length sequence corresponding to the respective analysis side ideal filters. Also the time domain analysis of this example is omitted because these ideal filters are of infinite length and it is difficult to explain every step using time domain analysis.

3.2 Equations governing 3 band perfect reconstruction filter banks

For simplicity in understanding I have redrawn the full filter bank diagram here

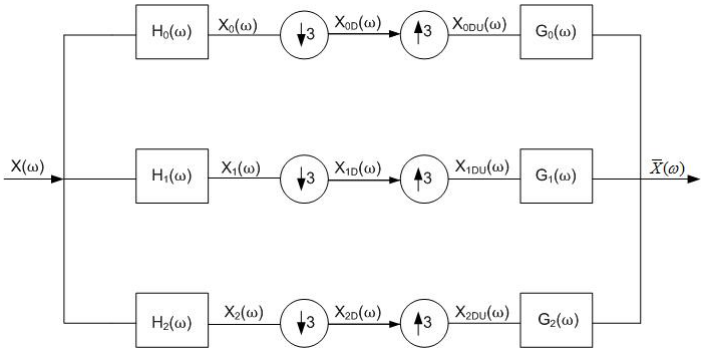

FIGURE 3.4: 3 band filter bank analysis

We know from ([1]:120) that any filter can be expressed in its polyphase form. Let H(z) be the set of analysis filters. $H(z) = [H_0(z)H_1(z)H_2(z)]^T$, which can be written as follows:

$$H(z) = \begin{bmatrix} E_{00}(z^3) & E_{01}(z^3) & E_{02}(z^3) \\ E_{10}(z^3) & E_{11}(z^3) & E_{12}(z^3) \\ E_{20}(z^3) & E_{21}(z^3) & E_{22}(z^3) \end{bmatrix} \begin{bmatrix} 1 \\ z^{-1} \\ z^{-2} \end{bmatrix} \tag{3.13}$$

$$H(z) \asymp E(z^3)e(z) \tag{3.14}$$

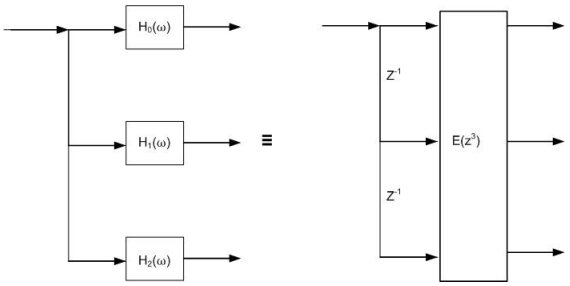

FIGURE 3.5: Pictorial representation of type1 polyphase decomposition

Let G(z) be the set of synthesis filters. $G(z) = [G_0(z)G_1(z)G_2(z)]$, which can be written as follows:

$$G(z) = \begin{bmatrix} 1 & z^{-1} & z^{-2} \end{bmatrix} \begin{bmatrix} R_{00}(z^3) & R_{01}(z^3) & R_{02}(z^3) \\ R_{10}(z^3) & R_{11}(z^3) & R_{12}(z^3) \\ R_{20}(z^3) & R_{21}(z^3) & R_{22}(z^3) \end{bmatrix} \tag{3.15}$$

$$G(z) \asymp z^{-2}e^T(z^{-1})R(z^3) \tag{3.16}$$

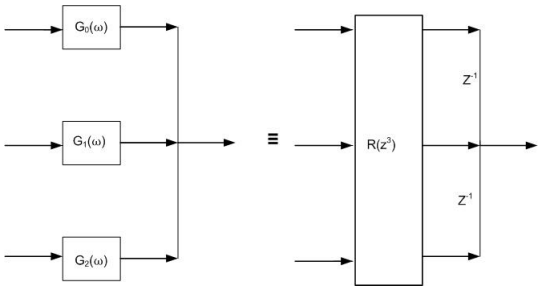

FIGURE 3.6: Pictorial representation of type2 polyphase decomposition

Using nobel identities and the polyphase decomposition, we can show that figure 3.1 can be redrawn as figure 3.7:

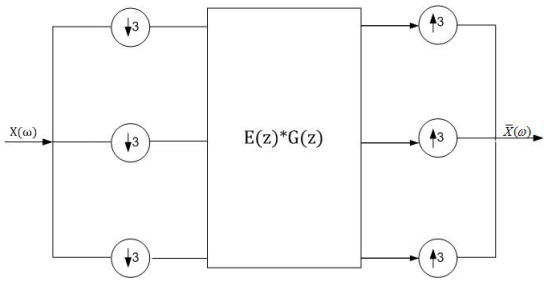

FIGURE 3.7: Equivalent system obtained after using nobel identities on filter banks structure

Hence if $R(z)E(z) = z^{-m}I$ (m is any finite integer), then we can have a perfect reconstruction since the remaining structure will then just be consisting of simple delays.

Necessary and sufficient condition for Perfect reconstruction of 3 channel FIR/IIR filters

$$R(z)E(z) = z^{-m}I \tag{3.17}$$

$$R(z)E(z) = z^{-m}\begin{bmatrix} 0 & I_{3-r} \\ z^{-1}I_r & 0 \end{bmatrix} \tag{3.18}$$

$$|R(z)||E(z)| = z^{-m} \tag{3.19}$$

For some integer $0 \leq r \leq 2$ and $m \in \mathbb{Z}$.
For practical purpose we consider finite impulse response filters. Hence this condition boils down to $|E(z)| = z^{-n}$ and $|R(z)| = z^{-k}$ for some integer n and k.

This structure also involves the inversion of $E(z)$ to get $R(z)$. This problem can be handled by avoiding the direct inversion of $E(z)$. This can be done by constraining $E(z)$ to be paraunitary (See Eqn. 4.9) (Paraunitary matrices have their determinant values $= z^{-n}$ with n as their McMillan degree).

Following is the example of a 3 channel FIR filter bank demonstrating this perfect reconstruction property.
One way to obtain a FIR E(z)satisfying the P.R condition is as follows :

$$E(z) = R_1 A(z) R_0 \tag{3.20}$$

$$A(z) = \begin{bmatrix} 1 & 0 & 0 \\ 0 & 1 & 0 \\ 0 & 0 & z^{-1} \end{bmatrix} \tag{3.21}$$

R_i is a constant nonsingular matrix. Let $R_0 = \begin{bmatrix} 1 & 1 & 3 \\ 0 & 1 & 0 \\ 1 & 1 & 1 \end{bmatrix}$ and $R_1 = \begin{bmatrix} 1 & 1 & 2 \\ 0 & 1 & 0 \\ 1 & 1 & 1 \end{bmatrix}$.

Hence,

$$E(z) = \begin{bmatrix} 2*z^{-1}+1 & 2*z^{-1}+2 & 2*z^{-1}+3 \\ 0 & 1 & 0 \\ z^{-1}+1 & z^{-1}+2 & z^{-1}+3 \end{bmatrix} \tag{3.22}$$

$$|E(z)| = 2*z^{-1} \tag{3.23}$$

The analysis filters are as follows :

$$H_0(z) = 1+2*z^{-1}+3*z^{-2}+2*z^{-3}+2*z^{-4}+2*z^{-5} \tag{3.24}$$

$$H_1(z) = z^{-1} \tag{3.25}$$

$$H_2(z) = 1+2*z^{-1}+3*z^{-2}+z^{-3}+z^{-4}+z^{-5} \tag{3.26}$$

$$R(z) = R_0^{-1}B(z)R_1^{-1} \tag{3.27}$$

$$B(z) = \begin{bmatrix} z^{-1} & 0 & 0 \\ 0 & z^{-1} & 0 \\ 0 & 0 & 1 \end{bmatrix} \tag{3.28}$$

$$R(z) = \begin{bmatrix} (z^{-1}+3)/2 & (-z^{-1})/2 & -z^{-1}-1.5 \\ 0 & z^{-1} & 0 \\ (-z^{-1}-1)/2 & (-z^{-1})/2 & z^{-1}+.5 \end{bmatrix} \tag{3.29}$$

$$|R(z)| = .5*z^{-2} \tag{3.30}$$

The synthesis filters are as follows :

$$G_0(z) = 1.5-1.5*z^{-2}+.5*z^{-3}-.5*z^{-4}-z^{-5} \tag{3.31}$$

$$G_1(z) = z^{-1} \tag{3.32}$$

$$G_2(z) = -.5+z^{-2}-.5*z^{-3}-.5*z^{-4}+z^{-5} \tag{3.33}$$

3.3 Cascade Algorithm

$a^0(n)$, $a^1(n)$ and $a^2(n)$ are the filter coefficients of an N length FIR analysis low pass, mid pass and high pass filter respectively. Respective dilation equation in terms of the scaling function will be as follows:

$$\phi(t) = \sum_{n=0}^{N-1} a^0(n) * \phi(3t-1) \tag{3.34}$$

$$\psi_1(t) = \sum_{n=0}^{N-1} a^1(n) * \phi(3t-1) \tag{3.35}$$

$$\psi_2(t) = \sum_{n=0}^{N-1} a^2(n) * \phi(3t-1) \tag{3.36}$$

Taking fourier transform on each side of above equation we get the following equation:

$$\hat{\phi}(\Omega) = \lim_{k\to\infty} \hat{\phi}(\Omega/3^k) \prod_{m=1}^{k} \left(\frac{1}{3}\right) * A^0\left(\frac{\Omega}{3^m}\right) \tag{3.37}$$

For finite Ω

$$\lim_{k\to\infty} \Omega/3^k = 0 \tag{3.38}$$

Therefore,

$$\hat{\phi}(\Omega) = \lim_{k\to\infty} \hat{\phi}(0) \prod_{m=1}^{k} \left(\frac{1}{3}\right) * A^0\left(\frac{\Omega}{3^m}\right) \tag{3.39}$$

(Eqn. 3.38) implies that scaling function $\hat{\phi}(\Omega)$ is a low pass function.

(Eqn. 3.37 - Eqn. 3.39) can be better understood from the figure 3.8:

Time domain equivalent :
The sequence $a^0(n)$ can thought of as a train of impulses at the integer locations (hence a continuous function). Lets call this continuous function as $a^0(t)$. Fourier transform of $a^0(t) \to \tilde{A^0}(\Omega)$. Hence,

$$a^0(3^m t) \to \frac{1}{3^m} * \tilde{A^0}\left(\frac{\Omega}{3^m}\right) \tag{3.40}$$

Taking the inverse fourier transform we get the following result

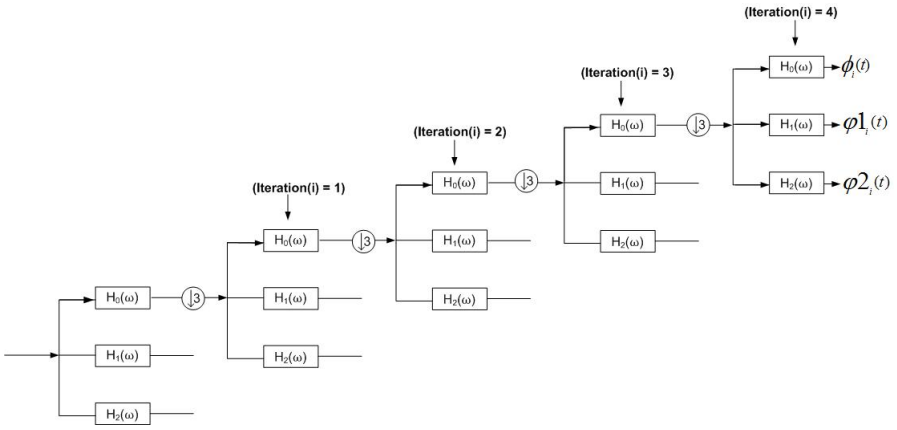

FIGURE 3.8: Equivalent system obtained after using nobel identities on filter banks structure

$$\phi(t) = \hat{\phi}(0) * \lim_{k\to\infty}((a^0(3t))\bigotimes(a^0(3^2t))\bigotimes\cdots(a^0(3^kt)) \tag{3.41}$$

$$\psi_1(t) = \hat{\phi}(0) * a^1(3t) * \lim_{k\to\infty}((a^0(3t))\bigotimes(a^0(3^2t))\bigotimes\cdots(a^0(3^kt)) \tag{3.42}$$

$$\psi_2(t) = \hat{\phi}(0) * a^2(3t) * \lim_{k\to\infty}((a^0(3t))\bigotimes(a^0(3^2t))\bigotimes\cdots(a^0(3^kt)) \tag{3.43}$$

In Practice we use only 7-8 iterations to get the scaling and wavelet functions, 3.9shows how after 7-8 iterations the shape of the functions don't change much.

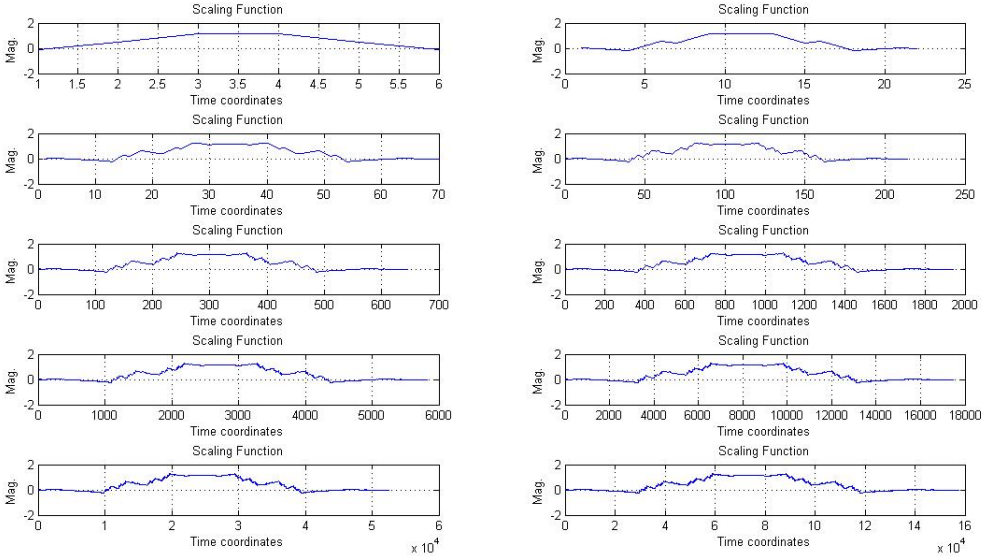

FIGURE 3.9: Equivalent system obtained after using nobel identities on filter banks structure

Chapter 4

Orthogonal Wavelet System

4.1 Parameterization of 3-band orthogonal wavelet system

The following section contains a complete parameterization for the 3- band compact wavelet system. Using the results filter banks are designed which on appropriate cascading gives the possible scaling and wavelet functions. The set of analysis filters can be written as:

$$a = \begin{pmatrix} a^0 \\ a^1 \\ a^2 \end{pmatrix} = \begin{pmatrix} a_0^0 & a_1^0 & . & . & a_n^0 \\ a_0^1 & a_1^1 & . & . & a_n^1 \\ a_0^2 & a_1^2 & . & . & a_n^2 \end{pmatrix} \tag{4.1}$$

where $a^0, a^1 and a^2$ are low pass(Scaling) , mid pass(Wavelet 1) and high pass(Wavelet 2) filter coefficients respectively

Using polyphase decomposition of type one ([13]: 23) we can express the impulse response of analysis filters as follows: for $s = 0to2, p[a]_k^s$ are the polyphase components

$$a^s(z) = \sum_{k=0}^{n} a_k^s(z^k) = \sum_{k=0}^{2} z^k p[a]_k^s(z^k) \tag{4.2}$$

where $s = 0to2$, $p[a]_k^s$ are the polyphase components

This gives us a matrix p[a](z), which we will refer to as polyphase matrix of

$$p[a](z) = \begin{pmatrix} p[a]_0^0(z) & p[a]_1^0(z) & p[a]_2^0(z) \\ p[a]_0^1(z) & p[a]_1^1(z) & p[a]_2^1(z) \\ p[a]_0^2(z) & p[a]_1^2(z) & p[a]_2^2(z) \end{pmatrix} \tag{4.3}$$

P[a](z)is called paraunitary ([1]:314), if

$$P[a](z) * P[a]^*(z^{-1}) = cI, where c is a nonzero constant and I is an Identity Matrix. \quad (4.4)$$

$P[a](z)$ is called 3-band orthogonal wavelet matrix if it satisfies:

$$P[a](z) * P[a](z^{-1}) = 3I \quad (4.5)$$

$$\sum_{k=0}^{2} p[a]_k^s(1) = \delta_{s,0} \quad (4.6)$$

Paraunitary property is very closely related to perfect reconstruction property . Equations 4.4 and 4.5 are the similarity between P.R and Orthogonal filter banks, where as 4.4 is the essential difference between them.

From the above mentioned equations in terms of the polyphase components we can deduce the following relation between the analysis filter coefficients:

$$EQN.\ 4.5 \Rightarrow \Sigma a_{k+3r}^{s_1} a_{k+3r_1}^{s} = \delta_{r,r_1}\delta_{s,s_1} \quad (4.7)$$

$$EQN.\ 4.6 \Rightarrow \Sigma a_k^s = 3\delta_{s,0} \quad (4.8)$$

Note: Our study and design will be restricted to the study of filters with length 3*k , for any positive integer k

From [9] we know that any polyphase decomposition P[a](z) of a 3 band orthogonal wavelet system that has length = 3*g and McMillan Degree = g-1, can be uniquely factorized as follows:

$$P[a](z) = V_{g-1}V_{g-2}V_{g-3}....V_1H_0 \quad (4.9)$$

$$V_k = [I - (1 - z^{-1})u_k u_k^T] \quad (4.10)$$

where u_k is any $3X1$ unit norm vector and H_0 is a real Haar Wavelet matrix

Chapter 5

TFP and Regularity Characteristics of Filter Banks

5.1 Method to generate highly localized wavelets

Uncertainty: A function and its Fourier transform, concurrently cannot be compactly supported Reference. Restricted by this constraint we move on to a relatively lesser limiting constraint of time and frequency variance of a signal, which can be compactly supported. Lesser the value of variance in a particular domain (time or frequency) the more compactly supported it is in that particular domain. The product of these time and frequency variance is called TFP (time frequency product) of Time Bandwidth Product. This product is a measure of the simultaneous compactness in both the domain. Uncertainty Principle: Product of time variance and frequency variance (T.F.P) of a function cannot be > 0.25. The theorem explains that after a certain degree of precision you cannot more finely resolve a signal simultaneously in time and frequency. Reference

In Literature there is very limited correlation developed between Time Bandwidth Product and other parameters like regularity (smoothness), convergence and frequency selectivity. By using a minimization algorithm, with TBP as the optimization function we try to get a correlation between TBP, regularity, frequency selectivity and convergence. Future parts ka Reference In theory, TBP is calculated both from frequency and time domain. Equations governing them are as follows: In time domain:

$$\sigma_t^2 = \frac{\int_{-\infty}^{\infty} t^2 |x(t)|^2 \, dt}{\int_{-\infty}^{\infty} |x(t)|^2 \, dt} \tag{5.1}$$

$$\sigma_\Omega^2 = \frac{\int_{-\infty}^{\infty} |dx(t)/dt|^2 \, dt}{\int_{-\infty}^{\infty} |x(t)|^2 \, dt} \tag{5.2}$$

$$TBP = \frac{\int_{-\infty}^{\infty} t^2 |x(t)|^2 \, dt}{\int_{-\infty}^{\infty} |x(t)|^2 \, dt} * \frac{\int_{-\infty}^{\infty} |dx(t)/dt|^2 \, dt}{\int_{-\infty}^{\infty} |x(t)|^2 \, dt} \tag{5.3}$$

In Frequency Domain:

$$\sigma_t^2 = \frac{\int_{-\infty}^{\infty} |\frac{d\hat{x}(\Omega)}{d\Omega}| d\Omega}{\int_{-\infty}^{\infty} 2 * \pi * |\hat{x}(\Omega)|^2 \, d\Omega} \tag{5.4}$$

$$\sigma_\Omega^2 = \frac{\int_{-\infty}^{\infty} \Omega^2 |\hat{x}(\Omega)|^2 \, d\Omega}{\int_{-\infty}^{\infty} |\hat{x}(\Omega)|^2 \, d\Omega} \tag{5.5}$$

$$TBP = \frac{\int_{-\infty}^{\infty} |\frac{d\hat{x}(\Omega)}{d\Omega}| d\Omega}{\int_{-\infty}^{\infty} 2 * \pi * |\hat{x}(\Omega)|^2 \, d\Omega} * \frac{\int_{-\infty}^{\infty} \Omega^2 |\hat{x}(\Omega)|^2 \, d\Omega}{\int_{-\infty}^{\infty} |\hat{x}(\Omega)|^2 \, d\Omega} \tag{5.6}$$

Method to calculate the Time Bandwidth Product for discrete signals:

1. Let us assume $f(n)$ is the function whose TFP value I need to calculate
2. I calculate the FFT of the normalized $f(n)$
3. The number of iterations used in cascade algorithm, provides us with the sampling distance in discrete time. (sampling time is inversely proportional to the 3^i, where i is the number of iterations)
4. The integrals involved in calculating the mean and variance (both in time and frequency domain) are calculated using the summations in the respective domains
5. Calculating the mean and variance in time domain is simply calculated using the summations
6. For the mean and variance in frequency domain, we first calculate the FFT of the sequence.
7. To calculate mean and frequency, we replace the variable Ω by an equivalent variable proportional to the FFT sequence index n. Ω is replaced by $2 * \pi * \frac{(n-1)}{N}$, where N is the Length of FFT

Procedure: Part 1 [understanding the TFP behavior for various input parameters]

1. Our aim is to find the effect these variables have on TFP value of the scaling and wavelet functions and eventually to have a set of input points that simultaneously gives high TFP localization of both the wavelets
2. The TFP calculations for length 6 filters involve 3 variables $var1, var2, Theta$. Amongst them we have shown earlier that does not change the value of TFP. Hence we are left with only 2 variables to deal with $var1, var2$

3. Hence, we create a grid of the first 2 variables $var1, var2$, where the axis of the grid is equally spaced samples of these 2 parameters
4. We calculate the TBP of the scaling and wavelet functions at all these points of the grid
5. Here we found 2 useful observation that we will use in our further investigation, they are:
   (a) The variation of the TBP values of the scaling and wavelet functions are same (as shown in figure: 5.1 and table: 5.1)
   (b) The variation of the TBP values of the scaling and wavelet functions repeat itself at regular intervals (as shown in figure: 5.2)

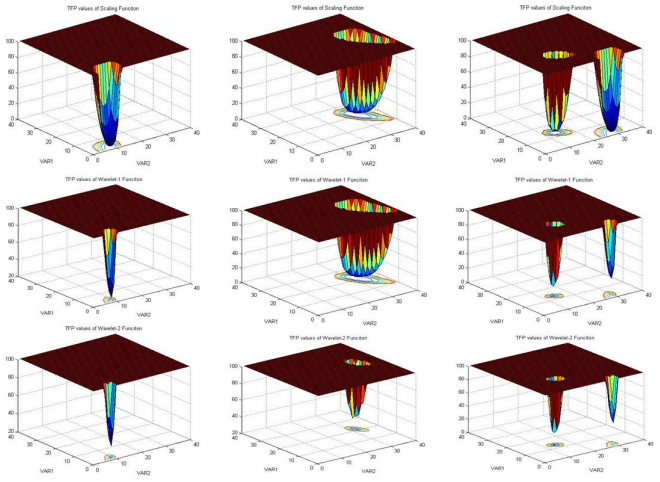

FIGURE 5.1: Similarity in Scaling and Wavelet Function TFP

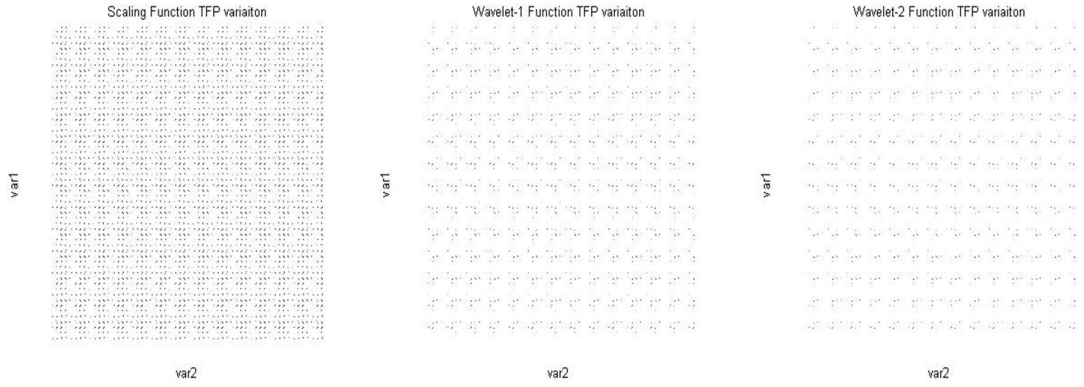

FIGURE 5.2: Similarity in TFP variation for both Scaling and Wavelet Functions

Procedure: Part 2 [calculating the input parameters that give highly localized wavelets] The aim of the next algorithm will be to calculate the minimum possible value of the sum of TFP of the 2 wavelets, we proceeded as follows:

1. We first create a cost function that calculates the sum of TFP values of the 2 wavelets
2. Since the TBP values of the wavelet functions repeats itself, we further divided the grid into 9 sub sections (shown in figure: 5.3)
3. For each subsection we make an even finer grid of $var1, var2$
4. At all points of this grid we calculated the TFP values and selected a set (S_1) of points that give us low TFP values (in our case this set is of 25 points, refer table: 5.2)
5. Individually, taking all the $var1, var2, Theta$ that correspond to these points(S_1) as the input parameter, we store the cost function and corresponding input variables as results for the particular grid
6. After calculating these results for all the 9 grids, we compare them and calculate the global minima of the as the point which corresponds to the least value of the $costfunction$

SUB GRID -1	SUB GRID -2	SUB GRID -3
SUB GRID -4	SUB GRID -5	SUB GRID -6
SUB GRID -7	SUB GRID -8	SUB GRID -9

FIGURE 5.3: Smaller Grids in which we will be working

*As we can see in GRID-1 that there are 2 minima each of which corresponds to a different input parameters and have different TFP values. This observation further supports our method of taking a set of points having less TFP sum of wavelets and then carries out the optimization algorithm for all of them.

5.2 Sobolev's Smoothness of Scaling Function

In the previous section, we have calculated that there is a high correlation between the properties of the scaling and wavelet functions. Hence now onwards we will study in

Correlation & Count → Function ↓	Count of Low TFP points	Correlation with Scaling function	Correlation with Wavelet-1 function	Correlation with Wavelet-2 function
Scaling function	4489	4489	1293	964
Wavelet-1 function	1293	1293	1293	964
Wavelet-2 function	964	964	964	964

TABLE 5.1: Correlation amongst TFP values of Scaling and Wavelet functions

	var1	*var2*	*Theta*	Scaling TFP	Wavelet -1 TFP	Wavelet-2 TFP	Sum TFP Wav-1 & Wav-2
GRID-1	-3.4736	-2.4712	0.5771	2.3981	12.3171	13.1788	25.4959
	-2.6908	-3.0832	1.1692	2.4050	13.2829	17.8599	31.1428
	-2.6908	-3.0832	1.1692	2.4050	13.2829	17.8599	31.1428
	-2.6908	-3.0832	1.1692	2.4050	13.2829	17.8599	31.1428
	-3.4736	-2.4712	0.5771	2.3981	12.3171	13.1788	25.4959
GRID-2	-0.4508	0.0584	1.1692	2.4050	13.2829	17.8599	31.1428
	-0.4508	0.0584	1.1692	2.4050	13.2829	17.8599	31.1428
	-0.4508	0.0584	1.1692	2.4050	13.2829	17.8599	31.1428
	-0.4508	0.0584	1.1692	2.4050	13.2829	17.8599	31.1428
	-3.5924	0.0584	1.1692	2.4050	13.2829	17.8599	31.1428
GRID-5	0.3320	0.6704	0.5771	2.3981	12.3171	13.1788	25.4959
	-0.4508	0.0584	-0.4016	2.4050	17.8599	13.1788	31.1428
	-0.4508	0.0584	-0.4016	2.4050	17.8599	13.1788	31.1428
	-0.4508	0.0584	-0.4016	2.4050	17.8599	13.1788	31.1428
	-0.4508	0.0584	-1.9724	2.4050	13.2829	17.8599	31.1428
GRID-7	-0.4508	-3.0832	1.1692	2.4050	13.2829	17.8599	31.1428
	0.4508	0.0584	1.1692	2.4050	13.2829	17.8599	31.1428
	-0.4508	0.0584	1.1692	2.4050	13.2829	17.8599	31.1428
	0.4508	-3.0832	1.1692	2.4050	13.2829	17.8599	31.1428
	0.4508	-3.0832	1.1692	2.4050	13.2829	17.8599	31.1428
GRID-9	0.3320	0.6704	0.5771	2.3981	12.3171	13.1788	25.4959
	0.3320	0.6704	0.5771	2.3981	12.3171	13.1788	25.4959
	0.3320	0.6704	0.5771	2.3981	12.3171	13.1788	25.4959
	0.3320	0.6704	0.5771	2.3981	12.3171	13.1788	25.4959
	0.3320	0.6704	0.5771	2.3981	12.3171	13.1788	25.4959

TABLE 5.2: Comparision of minimum TFP values for various small grids

only the scaling function and then generalize it for both wavelet and scaling functions. A function is said to be smooth if it is continuous and differentiable at all the points. Smoothness of a function is generally related with its regularity. A 3-channel finite impulse response (FIR) PUFB is said to be K-regular if and only if its scaling filter $H_0(z)$ has zeros of multiplicity K at the $K^(th)$roots of unity $e^(j*2m)/3)$,where $m = 0, 1, 2$.

A Similarly 3-channel PUFB is K-regular if and only if the band pass and the high pass filters have K multiple zeros at z=1. There is a close relation between regularity and the smoothness of the 3-band wavelet basis. The Sobolev regularity of a filter bank measures the L^2 differentiability of the scaling function which can be determined from the low pass filter $H_0(z)$.

Procedure:

1. Normalize $Q(z)$, such that $Q(1) = 1$
2. Calculate the convolution matrix of $Q(z) = T^Q$
3. The transition operator(T^Q) of $h(n)$ captures how the cascade algorithm converges and hence the stability of scaling function under iterations
4. Sobolev smoothness (S_max) is dependent on the spectral radius of T^Q
5. Smaller the spectral radius better is the sobolev smoothness

Results: Since the present research involves only length-6 filter banks. We will have only 1-regular filters. (Though 2 regular filters are also possible but upon searching for a solution for 2 regular filters in the given design I was getting no real solutions). With $Theta = \pi/9$ and var1 and var2 varying in a grid ($300x300$) of equally spaced points from $(0 - 2\pi)$. Following is the distribution of Sobolevs regularity:

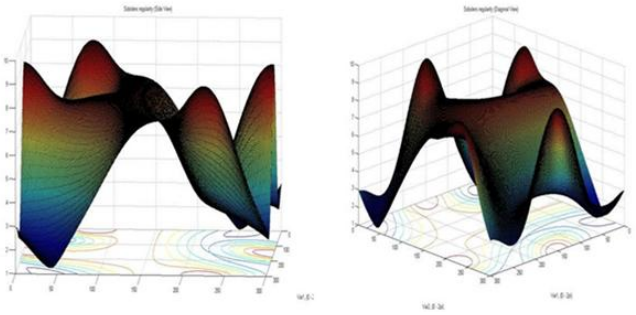

FIGURE 5.4: 3-D plot of Sobolev's regularity variation over the grid

5.3 New method to calculate the smoothness of scaling functions:

Carefully studying the scaling functions, I established a few smoothness characteristics of the functions and developed a method to select inputs which leads to smooth scaling

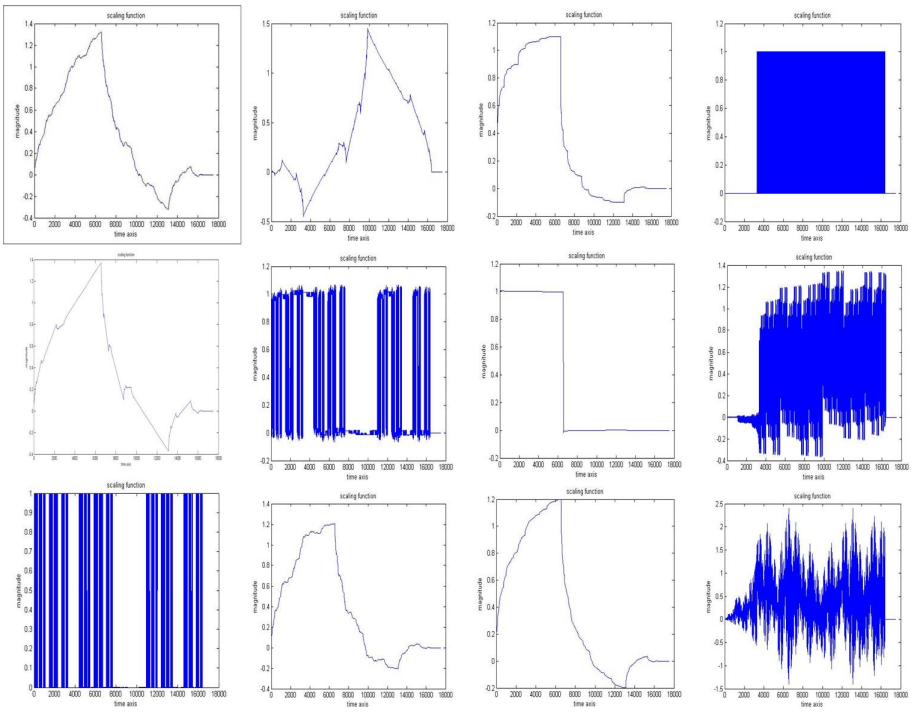

FIGURE 5.5: General Figures of the scaling filters

functions. Following are the examples demonstrating how the scaling functions vary for our system:

Following were the major characteristics of the scaling functions which reduce its smoothness:

1. A lot of small peaks
2. The surface is very rough, slope of the function is small but is changing very quickly
3. A single or multiple points where the function changes it values very quickly and the slope is high

To calculate the above 3 unwanted properties and to develop a cost function that measures the relative smoothness of a function, I adopted the following methods:

Let $f(n)$ be the curve in the discrete domain. Let $f^{''}(n)$ be the double differential of that curve and $|f^{''}(n)|$ be its absolute value Let $sf^{''}(n)$ be the sorted absolute values (descending order) of the double differential of the curve

Method 1: Double differential of a curve gives a measure of the change in slope, hence lesser the sum total of the absolute values of double differential, more will be the linear(almost constant slope) portions in the curve

$$cost1 = \sum_{n=1}^{N} |f''(n)| \tag{5.7}$$

Figure 5.6 is the curve that corresponds to the maximum smoothness according to this parameter. The circled regions are the point of concern (which we will refer to as small peaks) which dont get compensated by this cost function.

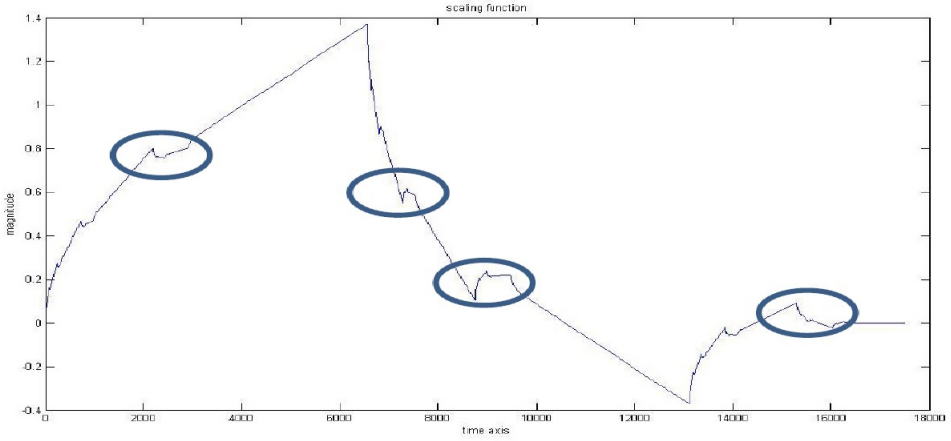

FIGURE 5.6: Most smooth plot when compared in the metric of cost1

Method 2: Sum of highest peaks (this no. is decided carefully upon selecting from a no. of values) of the double differential, a lesser no. of peaks implies that the function will not have high peaks, which may have had reduced its smoothness.

$$cost2 = \sum_{n=1}^{Threshold} |sf''(n)| \tag{5.8}$$

I have varied threshold from (.025 to .50 of the total) and then for these values subjectively analyzed the respective curves.

Figure 5.7 is the curve that corresponds to the maximum smoothness according to this parameter. The curve is very rough as compared to the other plots, though the slope is not changing drastically but it is changing at almost all points hence leading to this roughness.

Method 3: Number of small peaks (both shapes and), lesser is the peaks more smooth will be the function.

$$cost3 = countofsmallpeaks \tag{5.9}$$

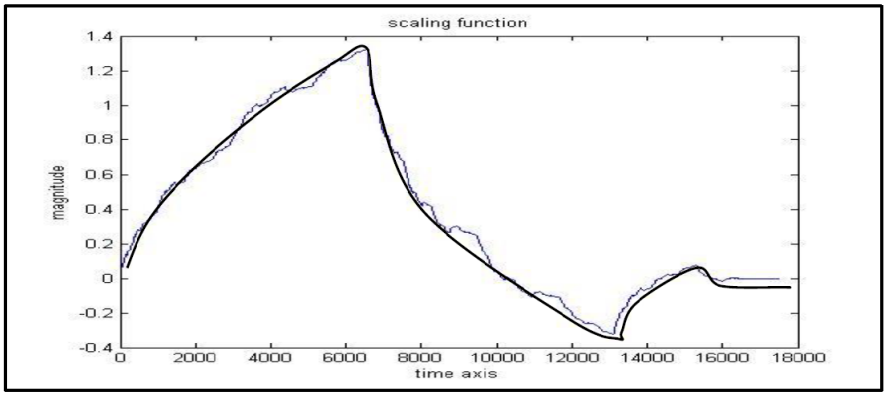

FIGURE 5.7: Most smooth plot when compared in the metric of cost2

Figure 5.8 is the curve that corresponds to the maximum smoothness according to this parameter. The function is not as rough as the previous one, but I have highlighted some portion in the curve which are still rough.

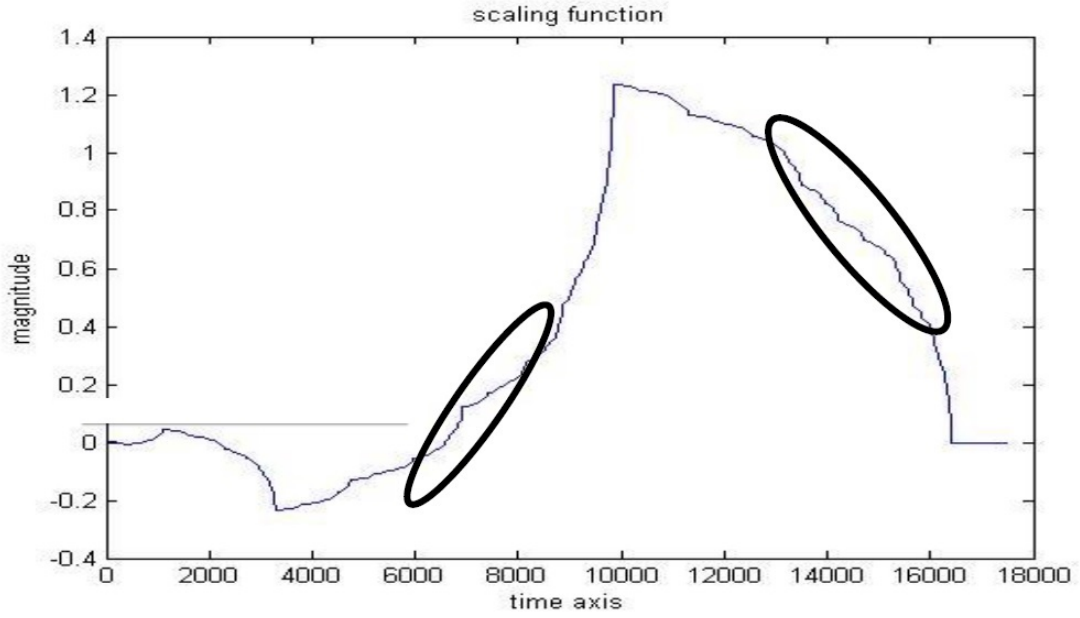

FIGURE 5.8: Most smooth plot when compared in the metric of cost3

All these cost functions have their own advantages and disadvantages, to get a curve that is smoother than all these 3 curves I need to have a cost function that contains the weighted sum of all these 3 cost functions, with the weights appropriately calculated.

Following will be the function:

$$costfunction = w1 * cost1 + w2 * cost2 + w3 * cost3 \tag{5.10}$$

The aim then becomes as to how decide what will be these weights w1,w2,w3. I have adopted the following method:

1. Decide the cost functions for the grid, and normalize them respectively
2. With the constraint w1+w2+w3=1, pick w1,w2,w3 from (.1,.2,.3,.4,.5,.6,.7,.8,.9,.99, .98,.97,.96,.95,.94,.93,.92) and calculate the $costfuntion$ for the grid
3. For a particular set of $w1, w2, w3$, calculate the input which gives the least value of cost function, where $costfunction = w1 * cost1 + w2 * cost2 + w3 * cost3$
4. For that particular input check what rank* does the corresponding scaling function has in the sorted $cost1, cost2, cost3$
5. Add the rank and the weight which gives you the least rank will correspond to the smoothest wavelet, which satisfies all the 3 conditions at the highest level

*rank: let suppose values of $cost1 = .1, .2, .3, .3, .4, .4, .4, .6$ and a scaling function has value of $cost1 = .6$ then its rank will be 5.

Results:

I have applied the above method for $Theta = \pi/2, \pi/3, \pi/4, \pi/6 and \pi/9$ and following were the results for the weights:

TABLE 5.3: Comparision of Weights for various Theta

$Theta \downarrow Weights \rightarrow$	W1	W2	W2
$\frac{\pi}{2}$	0.09	0.90	0.09
$\frac{\pi}{3}$	0.09	0.90	0.09
$\frac{\pi}{4}$	0.09	0.90	0.09
$\frac{\pi}{6}$	0.09	0.90	0.09
$\frac{\pi}{9}$	0.09	0.90	0.09

Since for different Theta I am getting the same weights, I will be using (0.09, 0 .90, 0 .01) as the weights in my function. With the above weight figure 5.9shows the variation of smoothness for the grid with $Theta = \pi/9$

This is very similar to the sobolev's smoothness plots 5.4

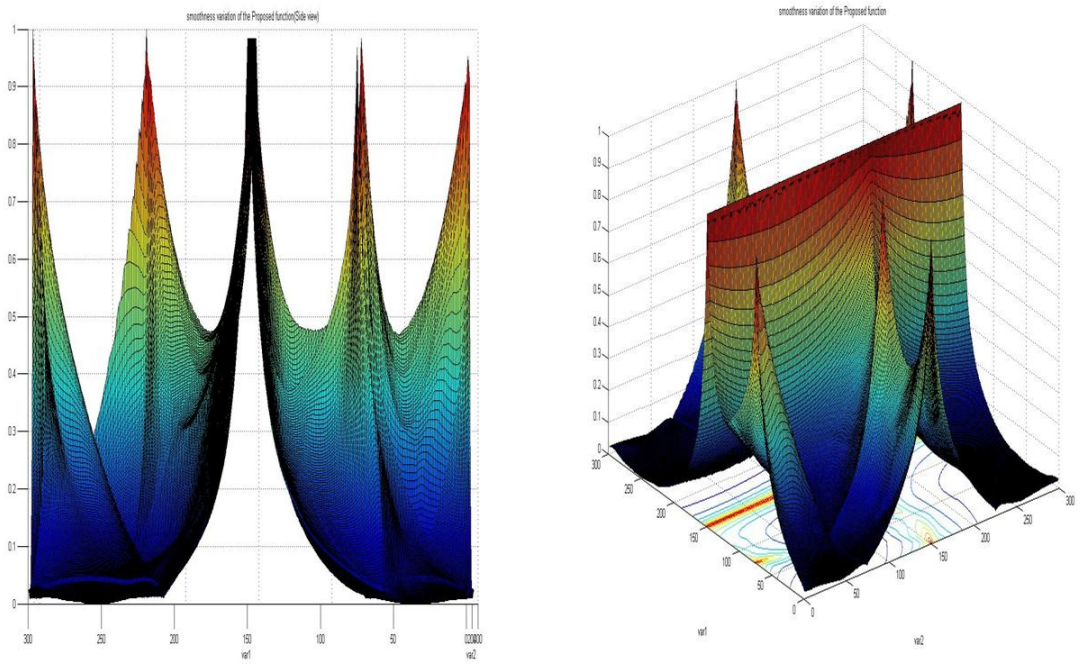

FIGURE 5.9: Regularity results for the grid with my cost function

Figure 5.10 is the comparision of the most smooth plots obtained from my method and sobolev's regularity.

Figure 5.11 is a comparision of the cummulative results:

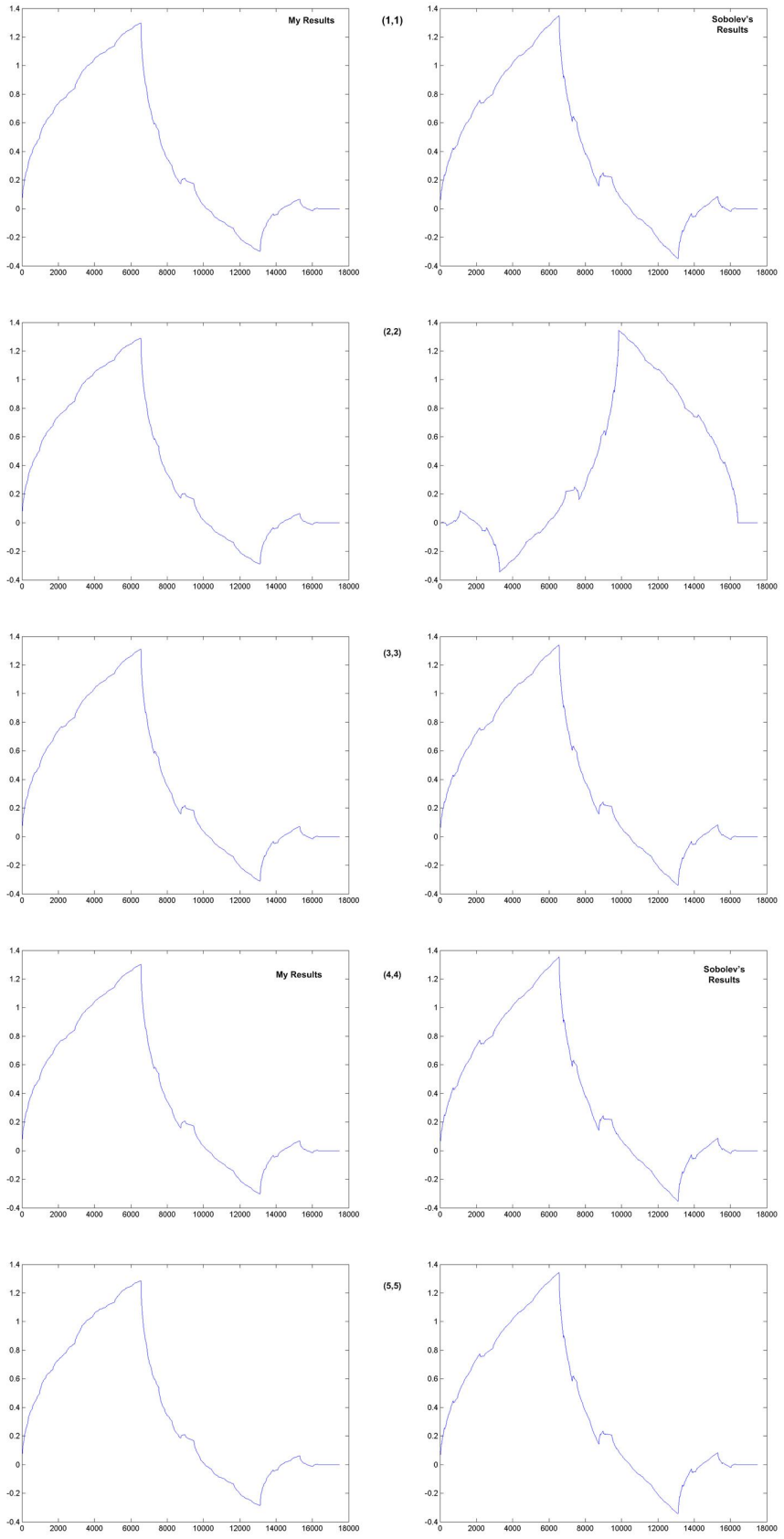

FIGURE 5.10: Regularity results for the grid with my cost function

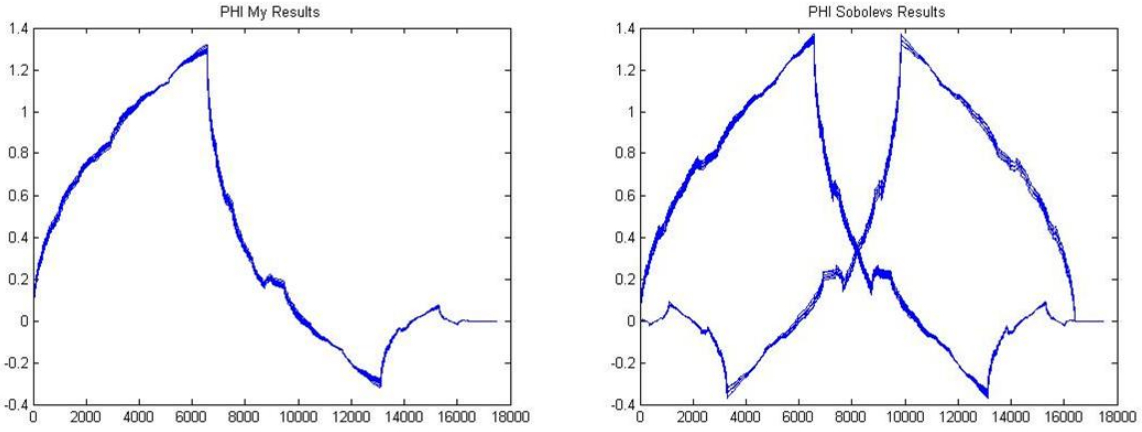

FIGURE 5.11: Regularity results for the grid with my cost function

Chapter 6

Conclusion and future work

Conclusion: In the first section of our investigation we have developed an algorithm through which, for a given parameterization of 3-band orthogonal wavelet system we were able to get the wavelets that were most highly localized in time and frequency domain. In the second section of our investigation we have developed a novel method to generate smooth scaling functions (as well as wavelet function). At a preliminary stage we have compared our results with the Sobolevs measure of regularity and we have found our results to be better than those obtained from his measure.

Future Work: In both the investigations there are a few areas which need to be explored before making a generalization of our results. For the TFP localized wavelets we need to implement a few more designs and verify our results for all of them. For the Smoothness criteria we can expand our research on generating the smoothness for filters of varied lengths and compare our results.

Bibliography

[1] P.P. Vaidyanathan, *Multirate Systems and Filter Banks*. New Delhi, India: Dorling Kindersley(India) Pvt. Ltd., 2006

[2] Ying-Jui Chen, Soontorn Oraintara, K.S Amaratunga, "Dyadic-based factorizations for regular paraunitary filterbanks and M-band orthogonal wavelets with structural vanishing moments," *Signal Processing, IEEE Transactions on* , vol.53, no.1, pp.193-207, Jan. 2005

[3] P. Steffen, P. N. Heller, R. A. Gopinath, and C. S. Burrus,"Theory of regular M-band wavelet bases," *Signal Process., IEEE Trans.*, vol. 41, no. 12, pp. 3497 - 3510, Dec. 1993

[4] R.A.Gopinath, C.S Burrus, "Factorization approach to unitary time-varying filter bank trees and wavelets," *Signal Processing, IEEE Transactions on* , vol.43, no.3, pp.666-680, Mar 1995

[5] Andre Tkacenko, P.P. Vaidyanathan, T.Q Nguyen, "On the eigenfilter design method and its applications: a tutorial," *Circuits and Systems II: Analog and Digital Signal Processing, IEEE Transactions on* , vol.50, no.9, pp.497 - 517, Sept. 2003

[6] Zou Hehong, A.H Tewfik, "Discrete orthogonal M-band wavelet decompositions," *Acoustics, Speech, and Signal Processing, IEEE International Conference on* , vol.4, no., pp.605-608, 23-26 Mar 1992

[7] Hui Xie, Joel M. Morris, "Design of orthonormal wavelets with better time-frequency resolution", *Proc. SPIE*, vol. 2242, no., pp. 878-887, 15 March, 1994

[8] Qingtang Jiang, "Orthogonal multiwavelets with optimum time-frequency resolution," *Signal Processing, IEEE Transactions on*, vol.46, no.4, pp.830-844, Apr 1998

[9] Peng Lizhong, Wang Yongge, "Parameterization and algebraic structure of 3-band orthogonal wavelet systems," *Science in China (Series A)*, vol. 44, no. 12, pp. 1531-1543, Dec. 2001

[10] Ritesh Kolte, Pushkar Patwardhan, Vikram M Gadre, "A class of time-frequency product optimized biorthogonal wavelet filter banks," *National Conference on Communications (NCC)*, vol., no., pp.1-5, 29-31 Jan. 2010

[11] Damiana Lazzaro, "Biorthogonal M-band filter construction using the lifting scheme," *Numeric Algorithms*, vol. 22, no.1, pp. 53 72, June 2006

[12] Ning Bi, Xinrong Dai, Qiyu Sun, "Construction of compactly supported M-Band Wavelets," *Applied and Computational Harmonic Analysis, vol.* , no., pp. 113-131, June 1995

[13] Tony Lin, Qingyun Shi, Pengwei Hao, "An Algebraic Approach To M-Band Wavelets Construction, not enough information available

[14] M. Vetterli, C. Herley, "Wavelets and filter banks: theory and design," *Signal Processing, IEEE Transactions on* , vol.40, no.9, pp.2207-2232, Sep 1992

[15] Martin Vetterli, Jelena Kovaevi, *Wavelets and Subband Coding*. Engelwood Cliffs, New Jersey: Prentice Hall of India Pvt. Limited., 1995

[16] M Smith, T.P Barnwell, "A procedure for designing exact reconstruction filter banks for tree-structured subband coders," *Acoustics, Speech, and Signal Processing, IEEE International Conference,*Vol.9,pp. 421-424,Mar. 1984

[17] P.P Vaidyanathan, P.Q. Hoang, "Lattice structures for optimal design and robust implementation of two-channel perfect-reconstruction QMF banks," *Acoustics, Speech and Signal Processing, IEEE Transactions on* , vol.36, no.1, pp.81,94, Jan 1988

[18] Oktay Alkin, Hakan Caglar, "Design of efficient M-band coders with linear-phase and perfect-reconstruction properties," *Signal Processing, IEEE Transactions on*, vol.43, no.7, pp.1579-1590, Jul 1995

[19] Anand K. Soman, P.P. Vaidyanathan, Truong Q. Nguyen, "Linear Phase Paraunitary Filter Banks: Theory, Factorizations and Designs," *Signal Processing, IEEE Transactions on* , vol. 41, no. 12, pp. 3480-3496, Dec. 1993

[20] G. Pau, B. Pesquet-Popescu, G. Piella, "Modified M-band synthesis filter bank for fractional scalability of images," *Signal Processing Letters, IEEE*, vol.13, no.6, pp.345-348, June 2006

[21] R.A. Gopinath, C.S. Burrus,"On upsampling, downsampling and rational sampling rate filter banks," *Signal Processing, IEEE Transactions on*, vol.42, no.4, pp.812 -824, Apr 1994

[22] J. Kovacevic, M. Vetterli, "Perfect reconstruction filter banks with rational sampling factors," *Signal Processing, IEEE Transactions on*, vol.41, no.6, pp.2047-2066, June 1993